

Formation of cavities in Si and their chemisorption of metals

D M Follstaedt and S M Myers

Sandia National Laboratories, Albuquerque, New Mexico USA 87185-1056

Abstract: Nanometer-size cavities formed in Si by He⁺ implantation and annealing are examined with cross-section TEM. During annealing at 700°C or above, He degasses from the specimens, leaving UHV cavities with reactive Si bonds on their walls. Cavity microstructures have been characterized in detail for an implanted fluence of 1×10^{17} He/cm². Cavity volume remains approximately constant (0.75 lattice sites/He) for anneals from 700 to ~1000°C, while surface area (3 to 7 times the wafer area) decreases with temperature as the cavities coarsen. The cavities are found to getter up to ~1 monolayer of Cu or Au from solution in Si without second-phase formation, thus identifying the trapping mechanism as chemisorption on the cavity walls.

1. Introduction

Bubbles are formed when semiconductors are implanted with He (Cullis et al 1978, Follstaedt et al 1992, Griffioen et al 1987). Since He is slightly permeable in Si the bubbles can be degassed by annealing, leaving nanometer-size empty cavities with surfaces as clean as those prepared in ultra-high vacuum. The cavities have been exploited to study the binding of H on their surfaces (Myers et al 1993), faceting and free energies of crystallographic planes (Cullis et al 1978, Follstaedt et al 1993, Eaglesham et al 1993), trapping of transition metal impurities (Follstaedt et al 1995, Myers et al 1995), and trapping of charge carriers at the dangling surface bonds (Seager et al 1994). In these studies, well characterized cavities with microstructures that can be manipulated are very useful; the cavities must also be relatively stable. Here we characterize cavity volumes and surface areas in detail using cross-section transmission electron microscopy (TEM). When Cu and Au are gettered to cavities from their equilibrium phases with Si, they saturate at amounts consistent with ~1 monolayer (ML) of solute on the cavity walls. Furthermore, TEM examination of cavities with trapped Cu show no precipitated phases. These findings lead us to conclude that the trapping is due to chemisorption of the metals on cavity walls.

Cavities were formed by ion implanting 1×10^{17} He/cm² at 30 keV into (001) float-zone Si. Cross-section TEM specimens were prepared using mechanical polishing and ion milling, as discussed elsewhere (Follstaedt et al 1992). Imaging was done with a Philips CM20T operating at 200 keV and capable of 0.27 nm resolution. To observe cavities in the midst of lattice damage from the implantation, specimens were tilted several degrees from the [110] orientation to reduce diffraction contrast from the damage, and cavities were imaged using underfocussing to highlight their edges with Fresnel contrast. In general, a greater underfocus (~1.5 μm) was required for optimum contrast with small cavities (~1 nm), lower magnifications (≤ 100 kx), or thick areas with high projected cavity densities, while less underfocus (~600 nm) was required when fewer, larger cavities (>~20 nm) were imaged, at higher magnification (≥ 200 kx), or in thin areas. Cavities were identified by their contrast change on going from underfocus (light inside/dark outside) to overfocus (dark inside/light outside). Cavities were counted and sized by their largest diameter, and their average area and volume were obtained from these distributions. The density of cavities per wafer area was obtained by measuring the specimen thickness using contours from two-beam diffraction conditions or Kikuchi lines in convergent-beam diffraction patterns (Kelly et al 1971).

DISCLAIMER

Portions of this document may be illegible in electronic image products. Images are produced from the best available original document.

Figure 1. Bright-field, cross-section TEM micrographs of Si implanted with 1×10^{17} He/cm² at 30 keV.

a) As implanted; imaged at $-1 \mu\text{m}$ (underfocus).

b) Annealed 1/2 hour at 700°C; imaged at $-1.2 \mu\text{m}$.

c) Annealed 1 hour at 900°C; imaged at -600 nm .

2. Cavity Microstructure Evolution

Figure 1a) shows the microstructure formed by implanting at room temperature with no anneal. A high density of 1-2 nm bubbles is found at depths of ~ 0.05 to $0.4 \mu\text{m}$; the density is highest at the He projected range, $0.3 \mu\text{m}$, where a peak concentration of 9 at.% He is predicted (Ziegler 1990). The dark contrast is a residual effect of the dense lattice damage, although individual dislocations were not resolved. Upon annealing the implanted Si for 1/2 hour at 700°C, the cavities enlarge to an average diameter of 8.5 nm and a well defined layer is found from 0.15 to $0.35 \mu\text{m}$, as in Fig. 1b). The overlayer is almost cavity-free. After 1 hour at 900°C larger (20 nm) cavities form, as in Fig. 1c). A few isolated dislocations can be seen with residual contrast in the images of annealed cavity layers. Numerous dislocations are found under two-beam conditions with low-index reflections. Annealed cavities often show facets, predominantly $\{111\}$, although many appear round. Some cavities are elongated along $\langle 111 \rangle$ directions and probably formed by coalescence. Detailed counting and sizing were done for three anneals as summarized in Table I. Cavity diameter increases with temperature and cavity density decreases, while volume remains approximately constant. The microstructure thermally evolves but the cavity layer persists, even after processing at 1180°C (Medernach et al 1995). The volume corresponds to 0.75 Si lattice sites per implanted He atom, suggesting that the He atomic density in bubbles approached that of a solid. It is notable that the $0.2 \mu\text{m}$ -wide cavity layer has a porosity of $\sim 7\%$. The internal cavity surface area is also high: 3 to 7 times the wafer area.

Table I. Summary of Cavity Microstructures and Surface Trapping Sites(001) Si implanted with 1×10^{17} He/cm² at 30 keV and subsequently annealed as indicated.

Anneal:	<u>½ hr. 700°C</u>	<u>1 hr. 800°C</u>	<u>8 hr. 800°C</u>	<u>1 hr. 900°C</u>	<u>½ hr. 1000°C</u>
Avg. Diameter (nm)	8.5	13.3	16	20	28
^a Areal Density of Cavities (cm ⁻²)	2.9x10 ¹²		6x10 ¹¹	3.1x10 ¹¹	
Cavity Volume per Wafer Area (nm ³ /nm ²)	12.4		16	15	
Cavity Area to Wafer Area Ratio	6.7		4.5	3.7	
^b Calculated Trap Sites per Wafer Area (cm ⁻²)	4.7x10 ¹⁵		3.2x10 ¹⁵	2.6x10 ¹⁵	
Trapped Solute per Wafer Area (at./cm ²)	4.8x10 ¹⁵ Cu		3.3x10 ¹⁵ Au	2.3x10 ¹⁵ Cu	

^a ±15% uncertainty in cavity density and related quantities.^b Cavity/Wafer Area Ratio multiplied by an areal density of 7 sites/nm².

3. Gettering Metal Impurities

We have investigated gettering of transition metals (Cu, Au, Ni, Co and Fe) to cavity layers and found them to be trapped strongly, with energies ≥ 1.5 eV with respect to solution (Follstaedt et al 1995, Myers et al 1995). The metals were introduced by ion implantation, annealed to form equilibrium phases, and their buildup at a separated cavity layer monitored with ion backscattering. Here we examine Cu and Au, which bind more strongly to cavities than the equilibrium phases and saturate the cavity sites. In a typical experiment, Cu₃Si was formed on one side of a wafer and cavities on the other; the Cu was gettered from the silicide across the wafer to the cavities during annealing at 600°C. The amount of trapped Cu increased with time and then saturated; 4.7×10^{15} Cu/cm² were found for cavities formed by annealing 1/2 hour at 700°C (Myers et al 1994).

The ratio of cavity area to the implanted wafer area can be used to predict the number of cavity-wall trapping sites per wafer area, assuming one metal atom per Si atom. The Si surface density differs for each facet plane; we use 7 Si bonds/nm², which is appropriate for unreconstructed {111} planes as well as 1x2 reconstructed {100} planes. The predictions are given in Table I along with the saturated amount of trapped Cu and Au found using cavities formed by annealing as indicated at the top of the table. Both metals saturate at levels consistent with 1 ML coverage of the cavity walls. The rather exact agreements are fortuitous given the 15% uncertainty in the area ratio and the use of a single surface density. Nonetheless, such agreement with two elements in several experiments with differing cavity areas is compelling support for chemisorption binding on cavity walls. Saturation at such low levels appears inconsistent with precipitation, which would probably continue until much of the implanted Cu (1×10^{17} Cu/cm²) was gettered to the cavities.

Cavities saturated with Cu were examined with TEM to look for precipitation directly. No evidence of second phases was observed in bright-field while tilting between high-symmetry directions nor in diffraction patterns. Moreover, only Si lattice spacings are seen in high-resolution (lattice) images, as in Fig. 2. Such images exhibit a contrast change between the interior and exterior of the cavity, but no indications of a second phase on the cavity walls are seen. The absence of Cu precipitation is readily understood, since silicide is already present and there is no thermodynamic driving force for additional precipitation. In some images, {111} atomic facet

Figure 2. High-resolution (lattice) image of a cavity from a layer in Si saturated with Cu. The cavity was formed by annealing 1 hour at 900°C and then gettering Cu for 26 hours at 600°C. Prominent facets are indicated.

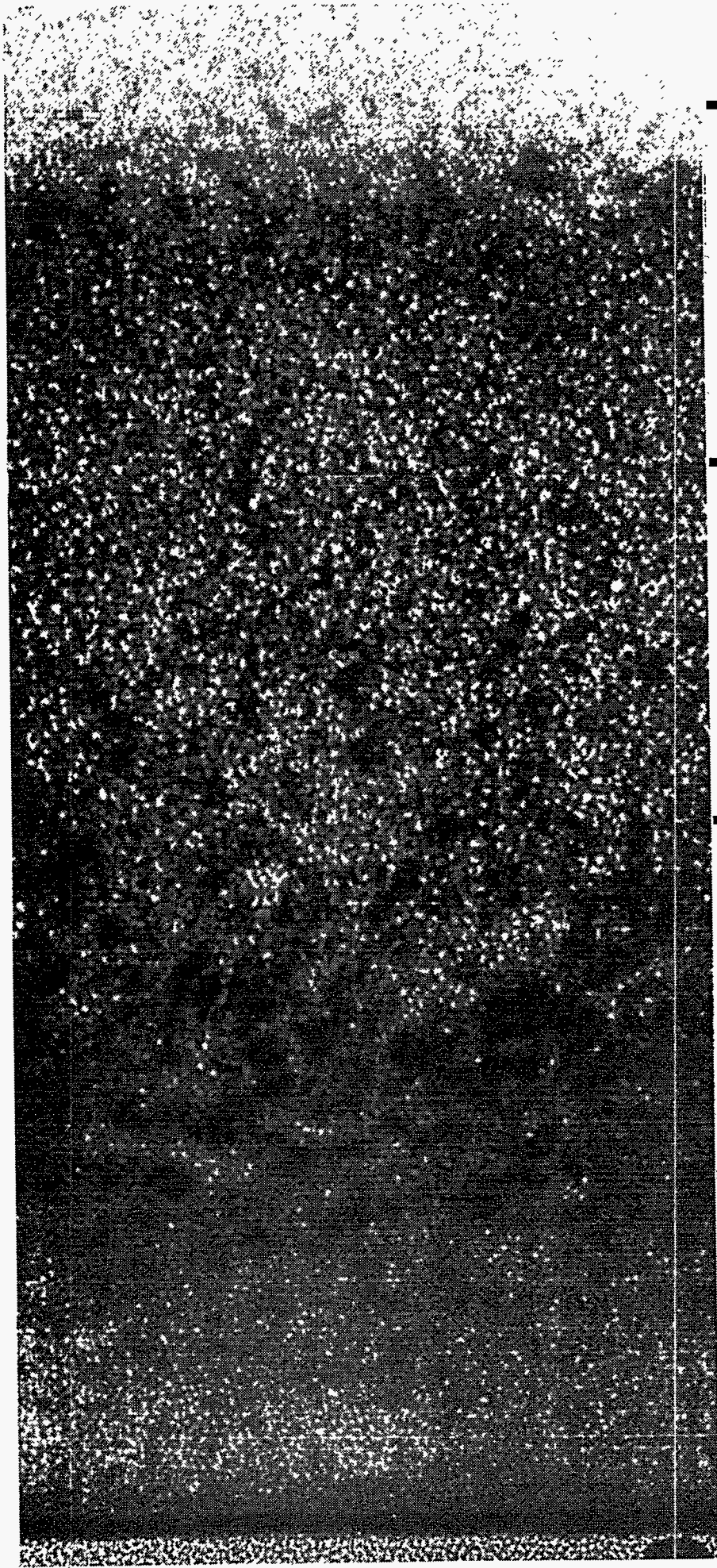
planes appears dark, which could be due to either Cu on the surface or surface reconstruction. In Fig. 2, flat {111} and {110} facets are readily identified. The cavity is also truncated in the (001) direction, but the surface rounds toward adjacent {111} planes as seen in pure Si (Follstaedt 1993). The images indicate that Cu binds on all three types of facets.

The binding energy of Cu (2.2 eV) to cavities has been used to model its gettering (Myers et al, 1994), and under representative technological conditions, the residual solution concentration could be reduced by several orders of magnitude more than achievable by precipitation-based gettering. Lower levels are achievable because the cavity gettering mechanism relies upon solute trapping which operates even at low concentrations, whereas precipitation can reduce concentrations only to the impurity solubility. Cavities appear viable as front-side gettering centers in future microelectronics devices, provided other detailed considerations are met (Medernach et al 1995).

This work supported by Division of Materials Sciences, Office of Basic Energy Sciences of the United States Department of Energy under contract DE-AC04-94AL85000.

4. References

- Cullis A G, Seidel T E and Meek R L 1978 *J. Appl. Phys.* **49** 5188.
Eaglesham D J, White A E, Feldman L, Moriya N and Jacobson D C 1993 *Phys. Rev. Lett.* **70** 1643.
Follstaedt D M, Myers S M, Wampler W R and Stein H J 1992 *Proceedings of the Electron Microscopy Society of America (San Francisco Press) Part I*, 334-335.
Follstaedt D M 1993 *Appl. Phys. Lett.* **62**, 1116.
Follstaedt D M, Myers S M, Petersen G and Medernach J 1995 *J. Electron. Mater.*, in press.
Griffioen C C, Evans J H, de Jong P C and Van Veen A 1987 *Nucl. Inst. Meth.* **B27** 417.
Kelly P M, Jostsons A, Blake R G and Napier J G 1975 *Phys. Stat. Sol* **a31** 771.
Medernach J W, Hill T, Myers S M and Headley T J 1995 to be published.
Myers S M, Follstaedt D M, Stein H J and Wampler W R 1993 *Phys. Rev.* **B47** 13,380.
Myers S M, Follstaedt D M, Bishop D M and Medernach J W *Semiconductor Silicon 1994*, eds H Huff, W Bergholz and K Sumino (Electrochem. Soc, Pennington, NJ) **PV94-10** 808.
Myers S M, Follstaedt D M, Petersen G A, Seager C H, Stein H W and Wampler W R 1995 *Nucl. Inst. Meth.* **B** in press.
Seager C H, Myers S, Anderson R, Warren W and Follstaedt D 1994 *Phys. Rev.* **B50** 2458.
Ziegler J F 1990 private communication.



0.4 μm

0.3

0.2

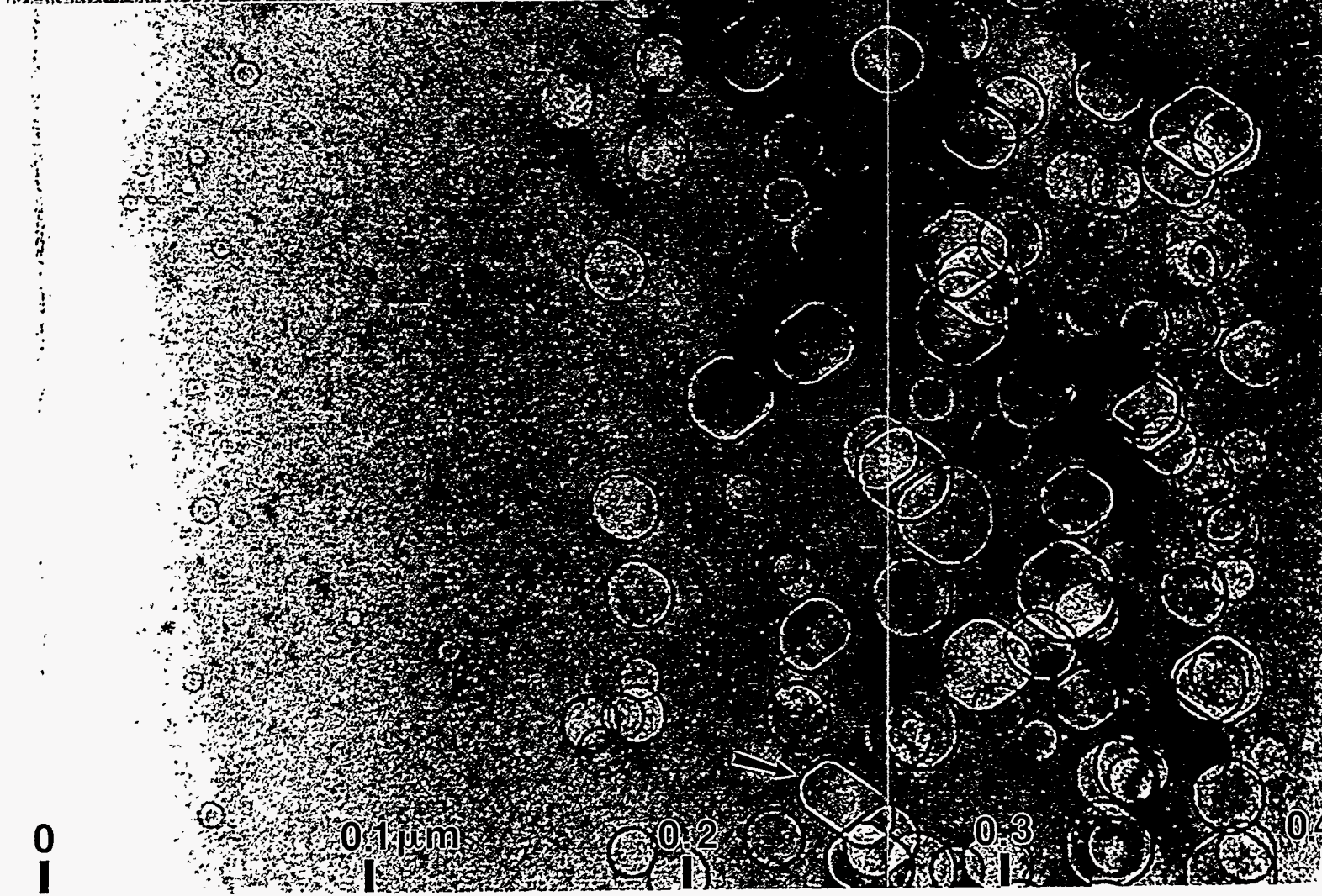
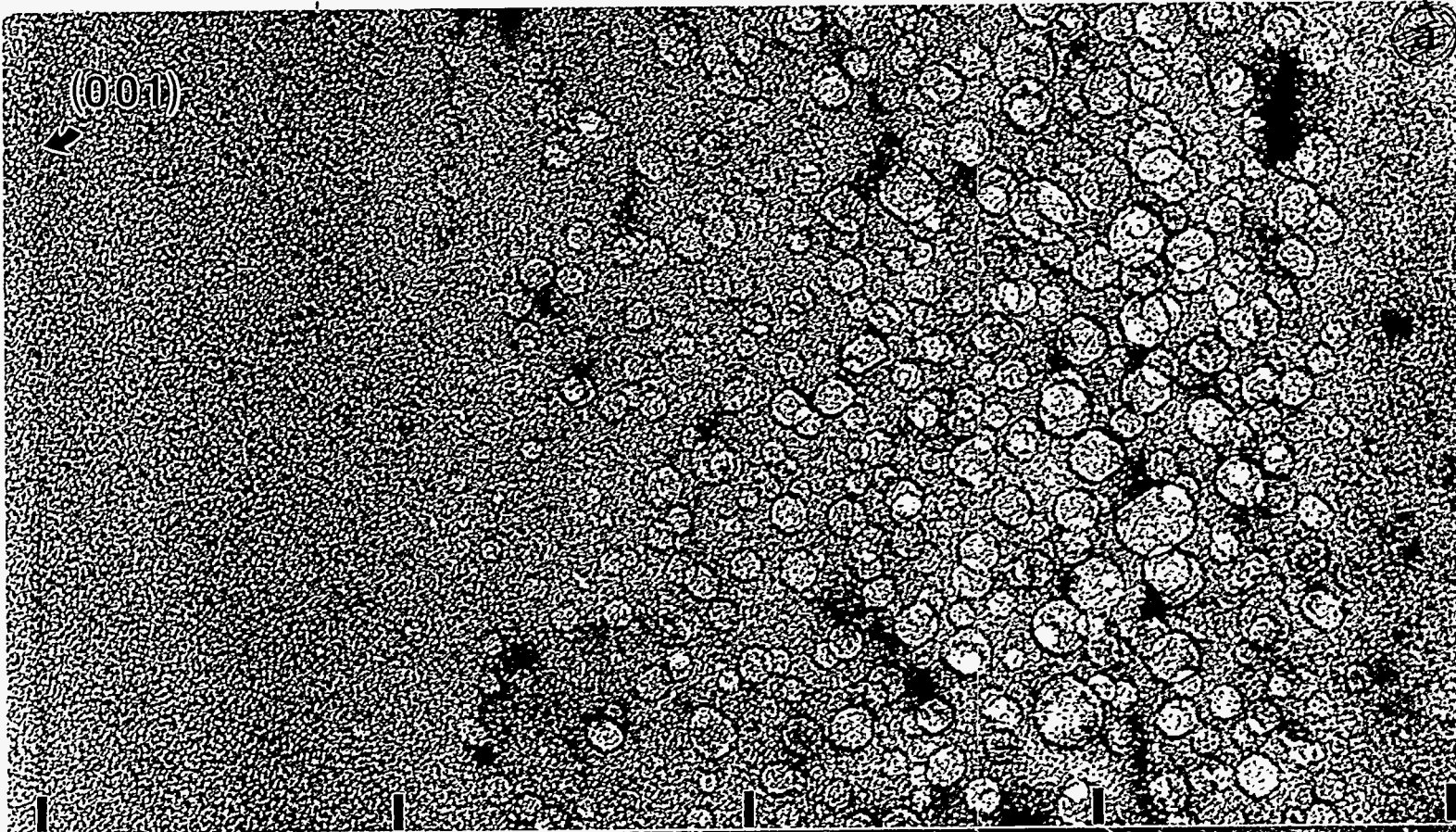
0.1

0

$1 \times 10^{17} \text{ He/cm}^2$ 30 keV
As Implanted

1a

(001)



0.1 μm

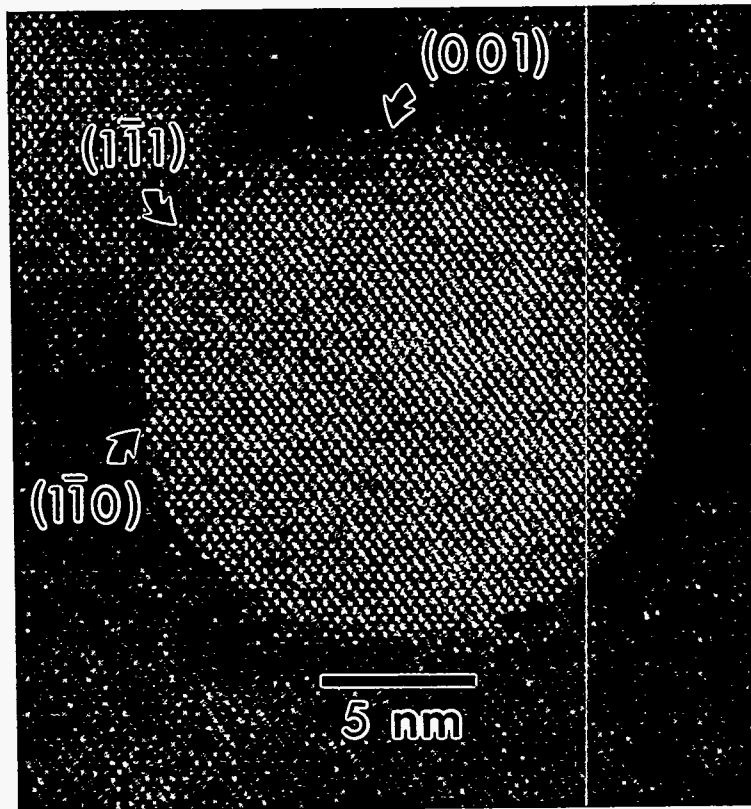
0.2

0.3

0.4

0

1c



2

DISCLAIMER

This report was prepared as an account of work sponsored by an agency of the United States Government. Neither the United States Government nor any agency thereof, nor any of their employees, makes any warranty, express or implied, or assumes any legal liability or responsibility for the accuracy, completeness, or usefulness of any information, apparatus, product, or process disclosed, or represents that its use would not infringe privately owned rights. Reference herein to any specific commercial product, process, or service by trade name, trademark, manufacturer, or otherwise does not necessarily constitute or imply its endorsement, recommendation, or favoring by the United States Government or any agency thereof. The views and opinions of authors expressed herein do not necessarily state or reflect those of the United States Government or any agency thereof.
